PHYSICAL REVIEW B **87**, 241202(R) (2013)

# Exciton interaction with a spatially defined charge accumulation layer in the organic semiconductor diindenoperylene

N. H. Hansen,[1,*] C. Wunderlich,[1] A. K. Topczak,[1,2] E. Rohwer,[3] H. Schwoerer,[3] and J. Pflaum[1,4,†]
[1]*Julius-Maximilians University, Am Hubland, 97074 Würzburg, Germany*
[2]*Center for Nanosystems Chemistry, Am Hubland, 97074 Würzburg, Germany*
[3]*Laser Research Institute, Stellenbosch University, Private Bag X1, Matieland, 7602 South Africa*
[4]*ZAE Bayern, Am Hubland, 97074 Würzburg, Germany*

(Received 21 February 2013; revised manuscript received 10 May 2013; published 18 June 2013)

We present an investigation of the microscopic interplay between excitons and charge carriers by means of combined photoluminescence (PL) and charge carrier transport measurements on organic thin film transistors (OTFTs). For this purpose, the prototypical organic semiconductor diindenoperylene was utilized as the active material. The OTFT accumulation layer provides a spatially defined interaction zone for charges and photogenerated excitons leading to a PL intensity reduction of up to 4.5%. This effect correlates with the accumulated hole carrier density and provides a lower estimate of about $1.1 \times 10^{-10}$ cm$^3$/s for the recombination rate of nonradiative exciton-hole processes. It is rationalized that these processes are preferentially mediated by trapped holes.

DOI: 10.1103/PhysRevB.87.241202 PACS number(s): 78.55.Kz, 72.20.Jv, 73.40.Qv

Excitons formed by electrostatically bound electron-hole pairs constitute fundamental excitations in organic semiconducting (OSC) materials. Generated either by photon absorption or by mutual capturing of charge carriers of opposite polarity, excitons play a key role in organic photovoltaic cells (OPVs) or organic light emitting diodes (OLEDs), respectively.[1–4] Conversely, exciton loss mechanisms corrupt the performance of optoelectronic devices and therefore have to be minimized.[5,6] Strong Coulomb-binding energies of up to 1 eV are able to stabilize paired electron-hole states in organic semiconductors against thermally activated dissociation, whereas interactions between excitons or with single charge carriers might lead to singlet exciton losses by various pathways, among which are exciton-exciton annihilation, where, by nonradiative recombination of one electron-hole pair, the remaining pair gains sufficient energy to overcome the Coulomb-binding energy required for dissociation, or charge carrier exchange accompanied by the formation of an energetically lower-lying triplet state.[7–9] Despite their importance, studies on the exciton loss mechanisms in technologically relevant thin films, together with an estimation of the pivotal recombination rates, are rather the exception, due to difficulties in precisely controlling the underlying boundary conditions, in establishing a spatially homogeneous interaction zone, and, finally, in achieving a response of suited amplitude to quantify the occurring loss processes.

In this Rapid Communication we focus on microscopic exciton quenching mechanisms induced by charge carriers and their investigation by photoluminescence (PL) quenching measurements on organic thin film transistor (OTFT) devices. This approach offers two essential advantages compared to studies on real optoelectronic devices or bulk single crystals. First, material inherent mechanisms can be identified without superimposed effects by locally inhomogeneous electric field distributions, induced, e.g., by nonideal heterojunction interfaces or space charging. Moreover, the choice of contact metal, in principle, enables the discrimination of recombination effects induced by electrons from those related to holes. Second, the tunable charge density in the TFT accumulation layer provides an additional degree of freedom to systematically influence charge carrier mediated exciton annihilation processes. Comparative studies of the PL quenching at different operational regimes of the transistor might unveil the origin of the participating charges, in particular, if they are free or spatially immobilized, e.g., by traps.

As an organic semiconducting material, the polyaromatic hydrocarbon diindenoperylene (DIP) was chosen. Besides its exceptional exciton diffusion properties in correlation with a long-range ordered thin film structure, which are necessary for the excitons to reach the accumulated charges, this compound has already been proven successful in OTFT applications as well as in photovoltaic cells.[10–13] Furthermore, the low optical absorption of DIP proves to be beneficial for the intended studies on the exciton-charge carrier interaction since it avoids pronounced quenching contributions by bimolecular recombination.

Thin film transistors were prepared in bottom-gate top-contact geometry as described by Klauk *et al.*[14] As illustrated in Fig. 1(a), a 60 nm thick aluminum film was evaporated under high vacuum (HV) (base pressure $10^{-6}$ mbar) at a rate of 1.8 nm/s on top of a Si wafer covered by 200 nm thick thermally grown $SiO_2$ (roughness below 0.4 nm). The native $AlO_x$. surface layer was further increased by oxygen plasma treatment, yielding a total thickness of 10.8 nm as confirmed by x-ray reflectivity (XRR) measurements. Thereafter, a homogenous and densely packed self-assembled monolayer (SAM) of pentadecylfluoro-octadecylphosphonic acid (FOPA) was grown overnight from a 2-propanol solution on top of the aluminum oxide. The effective FOPA film thickness of 2.2 nm has been verified by XRR measurements. The FOPA SAM enables reliable transistor operation in a voltage regime of up to 3 V and, even more important, its band gap of about 9 eV prevents injection of parasitic charges by the applied gate field or by the photoeffect (see below). Subsequent to gate preparation, DIP layers with thicknesses of up to 75 nm were grown by thermal evaporation under HV at a

 ©2013 American Physical Society

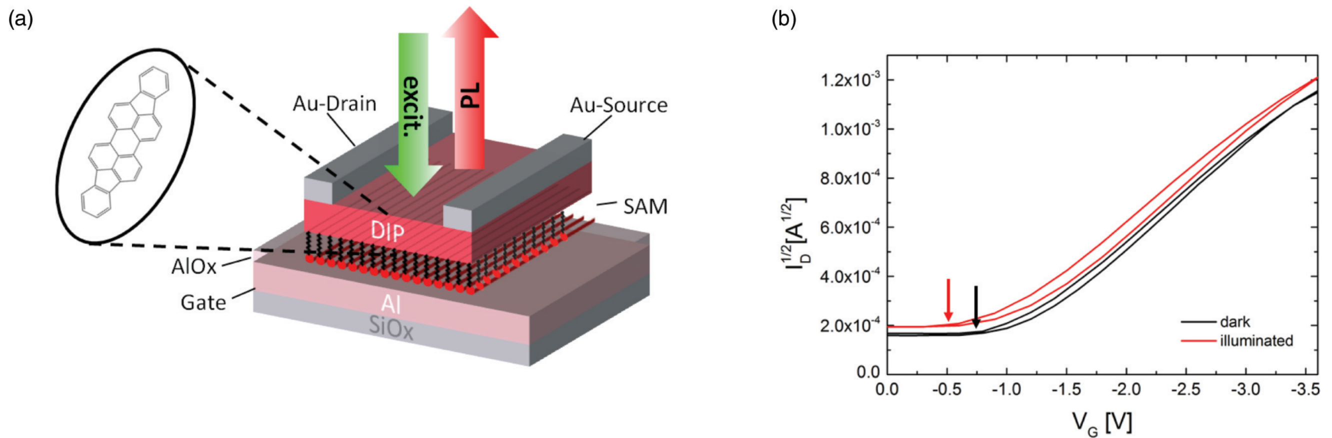


FIG. 1. (Color online) (a) DIP thin film transistor geometry, utilized for photoluminescence quenching studies. (b) OTFT transfer characteristics measured in the dark and under 532 nm illumination. As indicated by the arrows, a shift towards smaller threshold voltages occurs upon illumination whereas the absolute drain current remains almost constant (uncertainty of the data below 5%).

rate of 0.025 nm/s. The upper thickness limit was chosen according to x-ray diffraction studies, yielding a DIP crystallite extension along the surface normal, i.e., along the $c'$ direction, of similar size and therefore ensuring unhindered exciton transport along the vertical direction. Furthermore, assuming an index of refraction along the surface normal of $n_\perp = 1.7$, an optical excitation at $\lambda_{\text{exc}} = 532$ nm corresponds to an effective wavelength of $\lambda_{\text{eff}} = 300$ nm within the molecular layer. Thus, all DIP thicknesses studied comply with the condition $d_{\text{DIP}} < \lambda/4$ and, therefore, interference effects can be disregarded. Finally, the source and drain top contacts were made by 70 nm Au thermally deposited in HV at a fast rate of 2 nm/s to avoid metal penetration into the organic semiconductor layer underneath.[15,16]

To measure the voltage-dependent photoluminescence and, thereby, to estimate the amount of excitons quenched under charge accumulation, the DIP channel of the OTFTs was optically excited by a frequency doubled cw Nd:YAG laser ($\lambda_{\text{exc}} = 532$ nm) at a nominal power of 0.2 mW. The laser intensity remained constant during the transistor operation and was kept sufficiently low to guarantee a linear correlation with the generated exciton density, i.e., to avoid bimolecular contributions to the PL signal. This is corroborated by the fact that, assuming an exponential generation profile according to Lambert-Beer's law, at full power the two-dimensional (2D) projected area density of excitons amounts to at most $1/\mu\text{m}^2$, i.e., one exciton per $10^6$ DIP molecules, which yields an average exciton spacing substantially larger than the distance covered by the reported exciton diffusion length of about 100 nm along the $c'$ direction.[10] The PL emitted by the DIP transport layer was detected by a CCD camera [quantum efficiency (QE) > 90% in the measured spectral range] in combination with a spectrometer. To avoid degradation upon photoexcitation, all measurements on the organic layers have been performed under nitrogen atmosphere. At first, a PL measurement on the unbiased transistor was carried out as a reference for the subsequent studies at various $V_G$, i.e., various charge densities of the accumulated layer at the DIP/FOPA interface. To evaluate the PL emission at different regimes of TFT operation, the relative quenching $Q$, defined by the difference between PL at $V_G = 0$ ($\text{PL}^{nQ}$) and PL at $V_G \neq 0$ ($\text{PL}^{Q}$) normalized to the former, has been employed:

$$Q = 1 - \frac{\text{PL}^{Q}}{\text{PL}^{nQ}}. \quad (1)$$

Thus the relative quenching can be determined as a function of the gate voltage and consequently of the accumulated charge density using the areal capacitance $c_i = 0.44\ \mu\text{F/cm}^2$, which has been derived by the film thicknesses of the SAM (2.2 nm) and the $\text{AlO}_{x.}$ layer (10.8 nm) and assuming $\varepsilon_{\text{SAM}} = 2.5$ and $\varepsilon_{\text{AlO}_{x.}} = 9.4$ for the dielectric constants, respectively.

By determining the relative quenching the measurements become independent of the absolute PL intensity, which could differ for each sample, due to variation in the DIP film thickness. In addition, bimolecular processes as well as quenching at crystallographic defects such as grain boundaries or impurities are not accounted for by the relative measurement since they are equally present regardless of the applied gate voltage.

The 600 $\mu$m diameter laser spot was focused on the transistor channel ($L = 100$–$200\ \mu$m, $W = 1.5$ mm). Illuminated parts outside the accumulation zone contributed a voltage-independent background intensity of about 30% to the total PL signal at $V_G = 0$. We therefore consider the data deduced by PL quenching as a lower estimate. Prior to PL detection the equilibrium of charge distribution inside the DIP semiconducting channel was assured by sufficiently long delay and integration times during ramping of the applied voltage.

To evaluate parasitic charge generation by photorelease from the FOPA/$\text{AlO}_{x.}$ gate dielectric we compared the gate currents of transfer curves measured in the dark and under illumination, indicating no noticeable photogenerated charge contribution to the gate current. Furthermore, to identify effects by the concentration gradient and the diffusion of excitons in the organic transport layer, the PL quenching was investigated on OTFTs with different DIP layer thicknesses between 25 and 75 nm. No distinct influence of the exciton

diffusion could be observed, indicating this thickness regime to be smaller than the exciton diffusion length reported for DIP.[10]

The drain current increases upon illumination by 10% with respect to the current of 2 $\mu$A created by the field accumulated charges in the saturation regime. Furthermore, turn-on and threshold voltages, determined from the saturation regime, are shifted towards more positive values, as can be seen in Fig. 1(b). To appraise the influence of field induced exciton dissociation in the DIP channel, it has to be considered that any out-of-plane component of the electric field is compensated by the charge accumulation layer. Furthermore, the in-plane field between the source and drain of $F_{\max} = 2 \times 10^2$ V/cm is by far too small to compete with the critical field for exciton dissociation of $F_c = 5 \times 10^6$ V/cm, which has been derived using

$$F_c = \frac{E_B}{er}, \tag{2}$$

with a DIP exciton binding energy of $E_B = 0.5$ eV (Ref. 17) and a dipole extension of $r = 1$ nm; $e$ is the elementary charge. Therefore, field-assisted exciton dissociation can be discarded. Instead, we attribute the observed shifts to an increased hole injection into the organic semiconductor upon illumination, leading to an effective decrease in the trap density, as discussed by Orgiu *et al.*[18]

The PL intensity and its variation with gate voltage are displayed in the inset of Fig. 2 for a 60 nm thick DIP transistor channel. Accordingly, the relative quenching can be extracted at different drain voltages as a function of the applied gate voltage, as shown in Fig. 2. An almost linear increase of the relative quenching with gate voltage is apparent for small values of $|V_G|$, followed by saturation for $|V_G| \geqslant 1.6V$. In the following, we will denote the corresponding transition voltage as $V_{G,Q_{\rm sat}}$. In the saturation regime, the maximum quenching reaches up to $Q_{\rm sat} \approx 4.5\%$ and, therefore, provides an upper limit for nonradiative exciton-hole interaction with respect to the applied gate voltage.

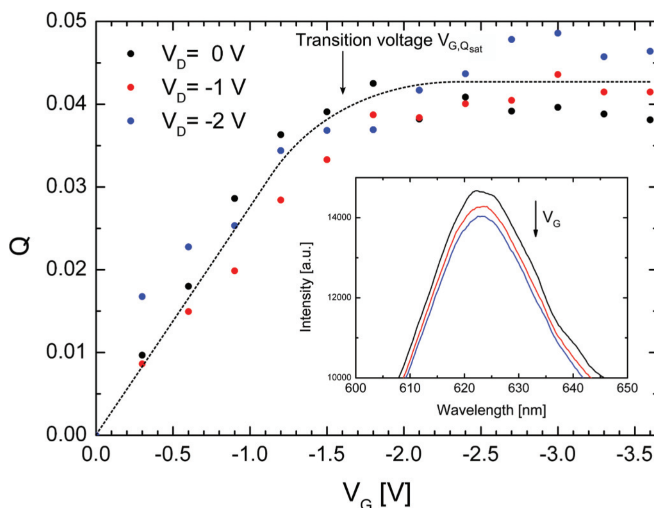


FIG. 2. (Color online) Relative photoluminescence quenching $Q$ of a 60 nm thick DIP transistor as a function of gate voltage $V_G$ for three different drain voltages $V_D$. The dependence of $Q$ on $V_G$, i.e., on the density of charges within the OTFT channel and its monotonous rise with increasing gate voltage, hints at the exciton interaction at the hole accumulation layer. The dashed line presents a guide to the eye to the data. The inset illustrates the effect of $V_G$ variation on the PL intensity of the DIP $S(1;0)$ transition. The decrease in peak intensity corresponds to an overall quenching of about 4.5%.

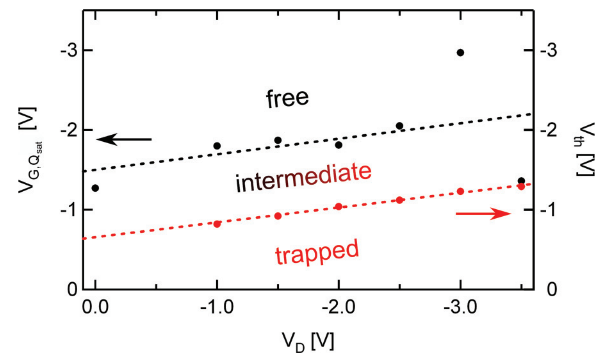


FIG. 3. (Color online) Threshold voltage $V_{\rm th}$ and transition voltage $V_{G,Q_{\rm sat}}$ under illumination as functions of the applied drain voltage. The slope of both quantities (dashed lines) is similar and indicates the same origin, namely, the density of occupied traps.

As the PL quenching increases linearly with gate voltage even above the threshold voltage, we can settle on the nature of charge carriers interacting with the photogenerated excitons. Up to the threshold voltage $V_{\rm th}$, the injected charges, in this case holes, become localized, i.e., their transport is significantly affected by trap states near the band edge. Due to the continuous filling of trap states upon lowering the Fermi level, traps behave energetically more shallow and therefore trapping becomes less efficient.[19] As the threshold voltage marks the transition region where most of the traps are filled and the injected holes behave as free charge carriers, we can relate the observed PL quenching mainly to localized, i.e., trapped, holes. To corroborate this model we compare the gate voltage required for quenching saturation $V_{G,Q_{\rm sat}}$ with the threshold voltage $V_{\rm th}$ under illumination at various drain voltages (Fig. 3 ). Both voltages increase linearly by a slope of 0.2, yet $V_{G,Q_{\rm sat}}$ is shifted towards more negative values by an offset of 0.8 V. Therefore, quenching is not only mediated by holes localized at deep traps for the entire gate voltage range but also by shallow trapped holes within a voltage regime of 0.8 V below $V_{\rm th}$. As soon as $V_{G,Q_{\rm sat}}$ is reached, additionally injected holes will be trapped on time scales being too short to contribute to the quenching. Hence, the increasing free charge carrier density does not significantly affect the quenching efficiency. Moreover, the similar slope of $V_{\rm th}$ and $V_{G,Q_{\rm sat}}$ as a function of drain voltage indicates the same origin for both transitions, namely, the increasing density of accumulated charges accompanied by a continuous filling of trap states. Our observation coincides qualitatively with previous fluorescence quenching studies on anthracene single crystals,[20] suggesting that an exciton interaction with trapped holes constitutes the major nonradiative loss channel, whereas PL decay remains constant upon an increase of the free charge carrier density. In contrast to this study, as well as to microwave conductivity measurements on disordered polymeric samples,[21] we are able to spatially control the

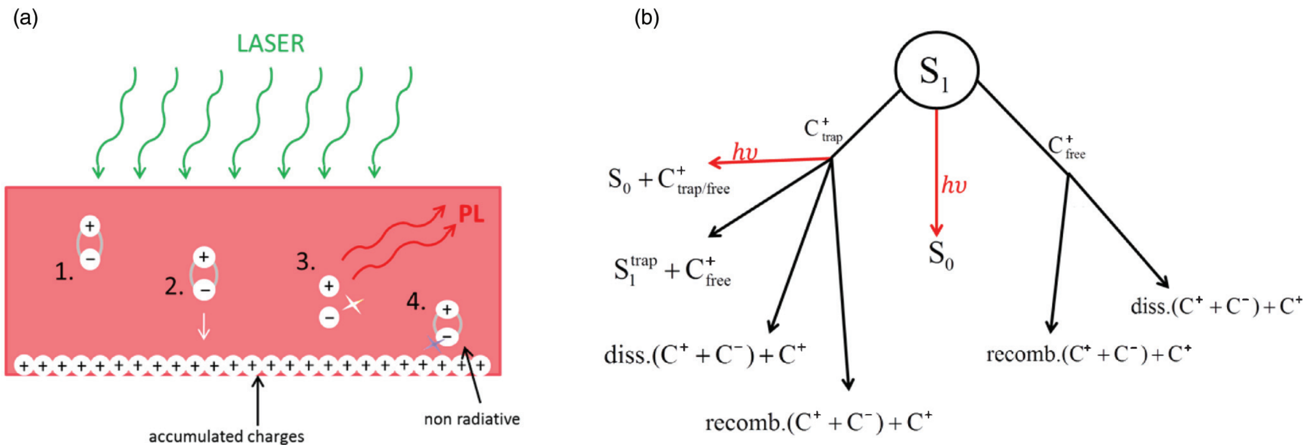


FIG. 4. (Color online) (a) Illustration of the relevant excitonic processes within the OTFT configuration. After photogeneration (1), exciton diffusion is steered by the concentration gradient towards the hole accumulation layer (2). Upon diffusion, either radiative recombination (3) or nonradiative processes (4), induced at the charge accumulation layer and yielding PL quenching, can occur. (b) Possible recombination scenarios leading to either PL emission (red arrows) or quenching (black arrows).

charge carrier density and to draw a direct correlation with the occurring fluorescence losses. Moreover, utilizing the OTFT accumulation zone for exciton-hole recombination allows us to distinguish precisely between effects caused by trapped and free charge carriers within a charge carrier concentration range of up to $10^{20}$ cm$^{-3}$.

To summarize the microscopic decay channels in more detail, Fig. 4(a) depicts the relevant exciton-related processes: First, an exciton is photogenerated upon light absorption within the DIP layer (step 1). Under steady-state conditions an exponential distribution of the exciton density will be established inside the organic layer. Second, within the concentration gradient, the exciton will diffuse to the charge accumulation layer (step 2) or radiatively recombine within its lifetime (step 3). However, if the exciton is able to reach the accumulation layer at the DIP/FOPA interface, it may recombine radiatively as well as nonradiatively (step 4). Possible recombination processes contributing to step 4 are listed in detail in Fig. 4(b). As we do not observe additional PL quenching contributions above $V_{G,Q_{sat}}$, i.e., when the density of free charge carriers is enhanced further, all quenching mechanisms based on the interaction between excitons and free holes can be disregarded [right branch of Fig. 4(b)]. Therefore, trapped holes can be identified as the primary source for nonradiative quenching of the photogenerated excitons [left branch in Fig. 4(b)].

Estimating a maximum concentration of $10^{-5}$ excitons per charge carrier for the applied laser intensity and with respect to the geometrical dimensions of the OTFT channel, we determined a lower limit for the effective exciton-hole recombination rate of

$$K = \frac{\Delta Q}{\Delta n_{\text{trap}} \tau_{\text{ex}}} = \frac{\Delta Q}{\Delta V_G c_i \tau_{\text{ex}}}, \tag{3}$$

with $\Delta Q/\Delta V_G$ describing the change in relative quenching upon variation of the gate voltage, while $\tau_{ex}$ is the exciton lifetime. To account for the conditions in our OTFT quenching experiments we have determined the exciton lifetime at room temperature by transient absorption measurements, yielding $\tau_{ex} \geqslant 1.2$ ns. Rationalizing that the excitons spend only a fraction of their lifetime inside the accumulation zone, we deduced a lower limit for the exciton-hole recombination rate of about $1.1 \times 10^{-10}$ cm$^3$/s. Though reliable data on this quantity are lacking for thin film systems so far, the comparison with single crystal PL quenching data, e.g., $8 \times 10^{-10}$ cm$^3$/s for naphthalene,[22] renders a sufficiently good agreement with our data. Therefore, estimation of this property by voltage-dependent luminescence quenching in thin film transistor devices provides a method that is applicable for a variety of luminescent compounds and for technologically relevant film thicknesses.

In summary, we presented an approach for the investigation of the exciton-charge carrier interaction in organic semiconductors. By utilizing TFT structures to create a well-defined charge carrier accumulation zone at the semiconductor/insulator interface, we measured the photoluminescence quenching as a function of the accumulated charge carrier density. In the course of these studies, two different quenching regimes could be identified where, from the linear regime, the quenching could be assigned to localized holes in the accumulation zone. From a maximum quenching efficiency of 4.5% we deduced a lower limit of the effective recombination rate for the exciton–localized hole interaction of about $1.1 \times 10^{-10}$ cm$^3$/s, which matches that reported for single crystals of low-weight molecules.

We gratefully acknowledge the generous financial support by the Bavarian State Ministry of Science, Research, and the Arts within the Collaborative Research Network "Solar Technologies Go Hybrid." This work was supported by the BMBF-Project GREKOS and the DFG-Project SPP1355.

*nhansen@physik.uni-wuerzburg.de

†jpflaum@physik.uni-wuerzburg.de

[1] M. Pope and C. E. Swenberg, *Electronic Processes in Organic Crystals and Polymers* (Oxford University Press, New York, 1999).

[2] P. M. Wiemer, A. Nenashev, F. Jansson, and S. D. Baranovskii, Appl. Phys. Lett. **99**, 013302 (2011).

[3] D. Coffey, B. Larson, A. Hains, J. B. Whitaker, N. Kopidakis, O. V. Boltalina, S. H. Strauss, and G. Rumbles, J. Phys. Chem. C **116**, 8916 (2012).

[4] V. Arkhipov and H. Bässler, Phys. Status Solidi A **201**, 1152 (2004).

[5] C. Deibel and V. Dyakonov, Rep. Prog. Phys. **73**, 096401 (2010).

[6] P. Heremans, D. Cheyns, and B. P. Rand, Acc. Chem. Res. **42**, 1740 (2009).

[7] A. J. Lewis, A. Ruseckas, O. P. M. Gaudin, G. R. Webster, P. L. Burn, and I. D. W. Samuel, Org. Electron. **7**, 452 (2006).

[8] M. A. Stevens, C. Silva, D. M. Russell, and R. H. Friend, Phys. Rev. B **63**, 165213 (2001).

[9] C. Gärtner, C. Karnutsch, and U. Lemmer, J. Appl. Phys. **101**, 023107 (2007).

[10] D. Kurrle, and J. Pflaum, Appl. Phys. Lett. **92**, 133306 (2008).

[11] A. C. Dürr, N. Koch, M. Kelsch, A. Rühm, J. Ghijsen, R. L. Johnson, J.-J. Pireaux, J. Schwartz, F. Schreiber, H. Dosch, and A. Kahn, Phys. Rev. B **68**, 115428 (2003).

[12] M. Horlet, M. Kraus, W. Brütting, and A. Opitz, Appl. Phys. Lett. **98**, 233304 (2011).

[13] A. Steindamm, M. Brendel, A. K. Topczak, and J. Pflaum, Appl. Phys. Lett. **101**, 143302 (2012).

[14] H. Klauk, U. Zschieschang, J. Pflaum, and M. Halik, Nature (London) **445**, 745 (2007).

[15] M. Schamberg, R. Adelung, and F. Faupel, Phys. Status Solidi A **205**, 578 (2008).

[16] M. Scharnberg, J. Hu, J. Kanzow, K. Rätzke, R. Adelung, F. Faupel, C. Pannemann, U. Hilleringmann, S. Meyer, and J. Pflaum, Appl. Phys. Lett. **86**, 024104 (2005).

[17] S. Krause, Ph.D. thesis, University of Würzburg, 2009, http://opus.bibliothek.uni-wuerzburg.de/volltexte/2009/4047/pdf/Diss_S_Krause.pdf.

[18] E. Orgiu, N. Crivillers, M. Herder, L. Grubert, M. Pätzel, J. Frisch, E. Pavlica, D. T. Duong, G. Bratina, A. Salleo, N. Koch, S. Hecht, and P. Samori, Nat. Chem. **4**, 675 (2012).

[19] G. Horowitz, P. Lang, M. Mottaghi and H. Aubin, Adv. Funct. Mater. **14**, 1069 (2004).

[20] N. Wotherspoon, M. Pope, and J. Burgos, Chem. Phys. Lett. **5**, 453 (1970).

[21] A. J. Ferguson, N. Kopidakis, S. E. Shaheen, G. Rumbles, J. Phys. Chem. C **112**, 9865 (2008).

[22] K. Nakagawa, M. Kotani, and H. Tanaka, Phys. Status Solidi B **102**, 403 (1980).